

Analysis of reentry vehicle flight dynamics

Yuriy Metsker^(†,‡), Klaus Weinand^(‡), Gregor Geulen^(‡), Oskar J. Haidn^(†)

^(†) Technische Universität München, Lehrstuhl für Flugantriebe

^(‡) MBDA Deutschland GmbH

Abstract

The knowledge of reentry vehicles (RV) flight characteristics regarding geometrical shape, dimensions and mechanical properties is essential for precise prediction of their flight trajectory, impact point and possible deviations according to simulation uncertainties. The flight characteristic estimations of existing RV require both – body dimensions and mechanical properties of the objects. Due to comparatively simple and reliable methods of specifying the vehicle outer dimensions, e.g. photos, video material, the estimation of mechanical properties is a subject of higher uncertainties. Within this study a medium range ballistic missile (MRBM) reentry vehicle was examined for several modifications, such as center of gravity position, weight moment of inertia, and initial reentry flight states. Combinations of these variables with constant aerodynamic properties for maximal lateral accelerations will be determined.

I Introduction

The development of missile defense systems requires sufficient knowledge about the flight behavior of designated target class at various reentry conditions. This information is used to determine necessary flight characteristics of the interceptor including required lateral acceleration capabilities, closing velocities and reaction dynamics, depending on engagement altitude. Especially the critical frequency variation of the vehicle during reentry may challenge the attitude control system of the interceptor, intending direct hits. Thus a generic reentry vehicle was designed to simulate maximal accelerations, critical frequencies and flight path deviations by variation of mechanical properties and reentry conditions. Additionally variations on range, flight time and approaching velocities were examined to verify the CEP of the impact.

II Case Study

II.1 Reentry Vehicle Parameters

The reentry vehicle examined in this study presents a typical payload for MRBM. The main characteristic of this class is the use of multiple stages with warhead separation after burnout of the second stage. Figure 1 shows dimensions of generic reentry vehicle. A non-maneuvering reentry vehicle will be assumed. The example which was chosen for the simulation is a two staged, solid propelled missile with total lift-off mass of ca. 21 [t]. Figure 2 and 3 show the flight and velocity profiles of this missile, simulated with an in-house software tool of MBDA GmbH^[1].

For a closer investigation, an altitude range between 40 and 30 km was selected as most interesting, due to low aerodynamic damping effects, resulting in relatively small incidence oscillation frequencies and consequently high trajectory deviations.

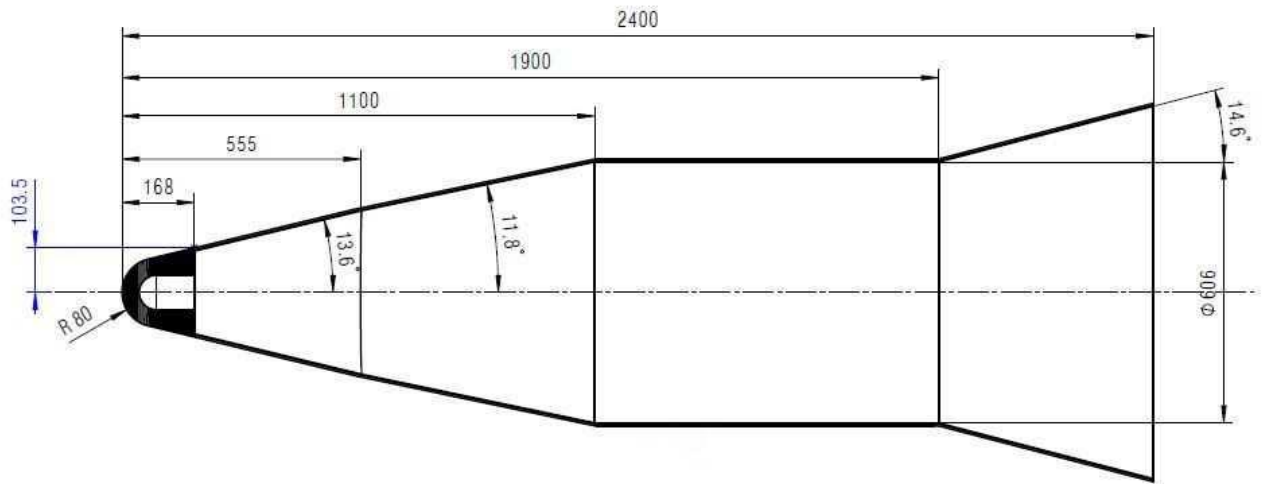


Figure 1: Reentry vehicle dimensions

General parameters of the reentry vehicle are summarized in Table 1.

Parameter	Value	Dimension
Total mass	740	kg
COG position (from cone)	1303	mm
I_{xx}	32,2	kg · m ²
$I_{yy} = I_{zz}$	224,8	kg · m ²

Table 1: Main parameter of the reentry vehicle



Figure 2: Flight profile of two stage ballistic missile

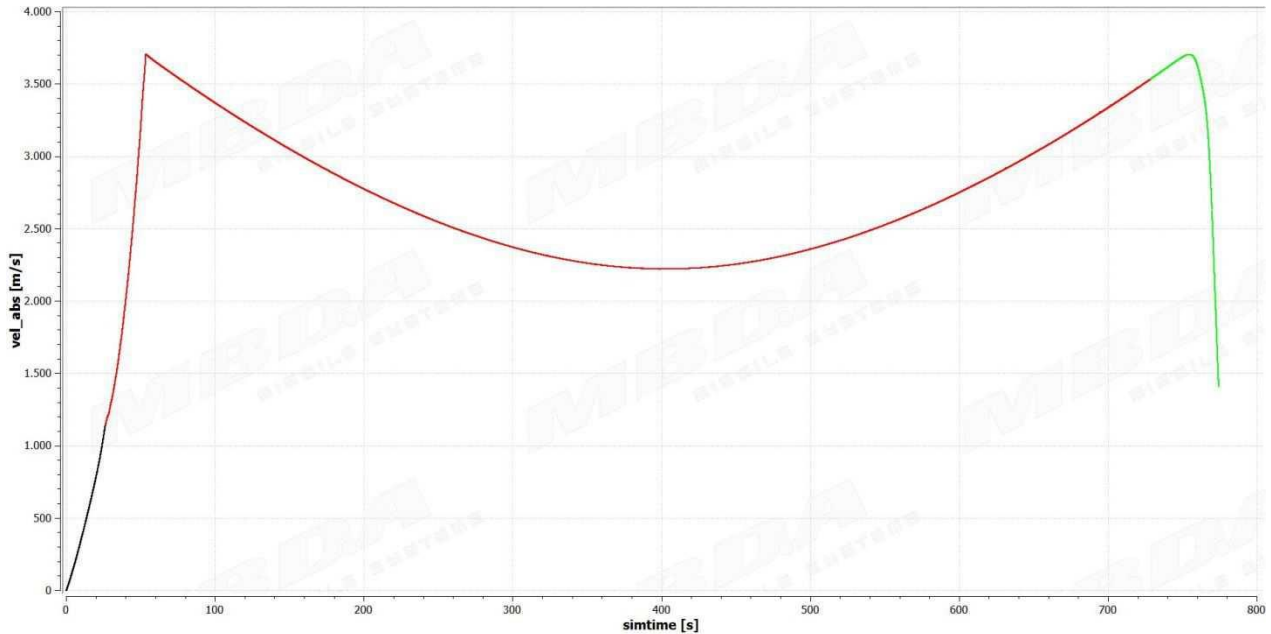


Figure 3: Velocity profile of two stage ballistic missile

II.II Simulation Tool

The simulations were performed by “threat analysis and simulation core” - software, designed within MBDA GmbH. State of the art earth gravity – EGM96 and climate/atmosphere MSIS-E-90 models for global simulation were used. The software works with a sophisticated boost and thruster model to represent characteristic parameters of several specified rocket engines. The core is capable to simulate multiple objects concerning continuous velocity variation during the ballistic reentry, depending on adaptable aerodynamic data quantity and quality. For simulation of reentry vehicles, full 360° of freedom CFD aerodynamic data bases were calculated and implemented. The complete simulation timing is adjustable to fulfill real-time requirements or demands for higher precision or runs. In the current study, simulations were made with 2 kHz frequency.

At reentry velocities over ca. 4000 m/s ionization effects due to aerodynamic and thermodynamic coupling may occur ^[2,3]. This results in boundary layer variation of the reentry vehicle, affecting deviation between real circumstances and CFD simulations. Nevertheless expected velocities during the reentry of MRBM warheads, yield in current simulation ca. 3600 - 3800 m/s, where ionization effects may be neglected.

II.III Reference simulation and variation cases

Due to high data workload for a simulation with the complete flight endurance, it is more favorable to analyze only the reentry maneuver with an appropriate variation of initial parameters. For the simulations a reentry site was selected over the Mediterranean Sea with the following initial reference parameters:

Initial Parameter	Value	Dimension
Inclination angle γ_0 :	-38	[°]
Start altitude h_0 :	120	[km] over MSL
Angle of Attack α :	0	[°]
Velocity v_0 :	3600	[m/s]
Roll rate p_0 :	0	°/s
Velocity Azimuth:	90	°

Table 2: Initial reference parameters of the simulation

No changes to the reference mechanical settings as mentioned in Table 1 were made. Figure 4 shows the reference reentry trajectory:

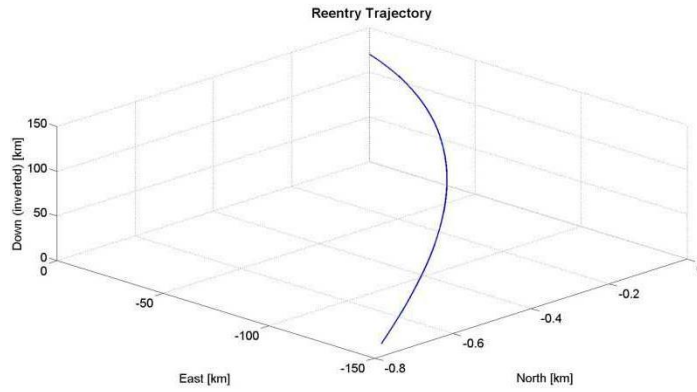


Figure 4: Reference simulation trajectory

Due to trimmed flight parameters, only small oscillations of the aerodynamic angle of attack occur, e.g. Figure 5. Yaw angle oscillations are located at similar small values.

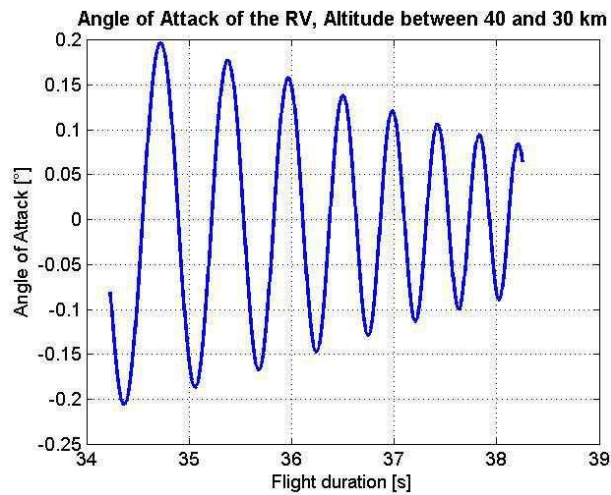


Figure 5: Angle of attack within considered altitude

Due to the absence of roll inducing moments, the acceleration values are not symmetrical to the origin of coordinates and are dominated by earth gravity and small aerodynamic drag, resulting from angle of attack oscillations. Figure 7 shows typical values of acceleration and velocity profiles at altitudes between 40 and 30 km. Lateral acceleration results from external aerodynamic forces taking into account round, rotating earth.

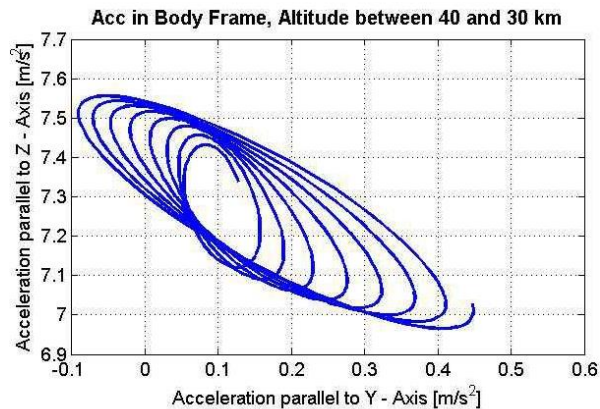


Figure 6: Acceleration in reference case, plane normal to undisturbed trajectory

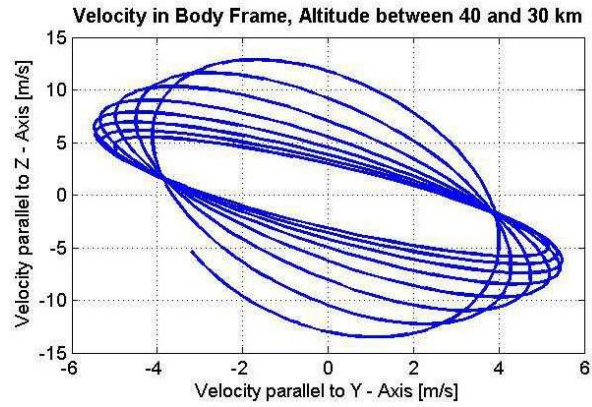


Figure 7: Velocity in reference case, plane normal to undisturbed trajectory

Integration of the lateral velocities without considering reference frame transformation, yields typical deviation history as pictured in Figure 8.

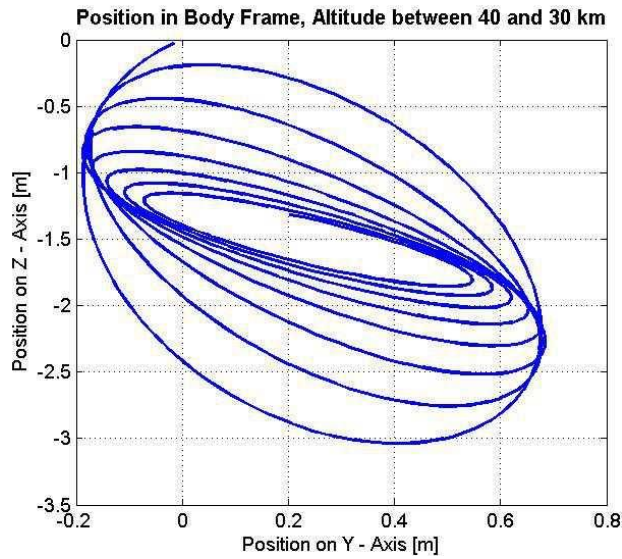


Figure 8: Side location, plane normal to undisturbed trajectory

The total displacement of the trajectory may be determined by observing the position in the NED frame, see Figure 9. Here two points on the flight trajectory at the beginning and end of a specified altitude are selected and reference line of sight with calculation of normal distances to trajectory points is build. The total deviation is characterized by the curvature of the trajectory, influenced rather by earth gravitation, then by aerodynamic effects. Obviously effects from small aerodynamically induced oscillations and hence accelerations shown in Figure 7, which occur at frequencies of 1.5 – 2 Hz, have no major impact.

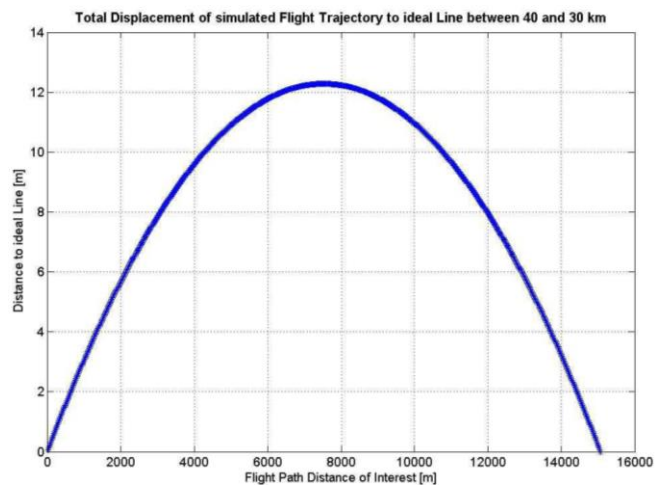


Figure 9: Total displacement of simulated flight trajectory to ideal line

III. Analysis of parameter modification

Reverse engineered reentry vehicles with well estimated contour still show uncertainties in determination of their real aerodynamic coefficients, total mass, COG position, moments of inertia as well as possible initial flight condition given by the post boost system. Variation of these parameters will be observed, discussed and compared to reference simulation case ^[4].

III.1 Variation of aerodynamic coefficients / derivatives

Aerodynamic coefficient variations may occur by modelling inaccuracies, overseeing small aerodynamic surfaces, assumed area roughnesses or dimensions.

Coefficients with major impact as defined in Table 3 ^[5] were varied by $\pm 50\%$ with an increment of 2%.

C_A	Axial force coefficient
C_N	Normal force coefficient
C_m	Pitching moment coefficient
C_{lq}	Roll damping coeff. due to pitch rate
C_{mp}	Pitch damping coeff. due to roll rate
C_{nr}	Yaw damping coeff. due to yaw rate

Table 3: Aerodynamic coefficients

Due to a time-discrete calculation of aerodynamic coefficients within the simulation, these were multiplied each time step by a gain factor. The reference simulation has an amplification factor of 1 in each case.

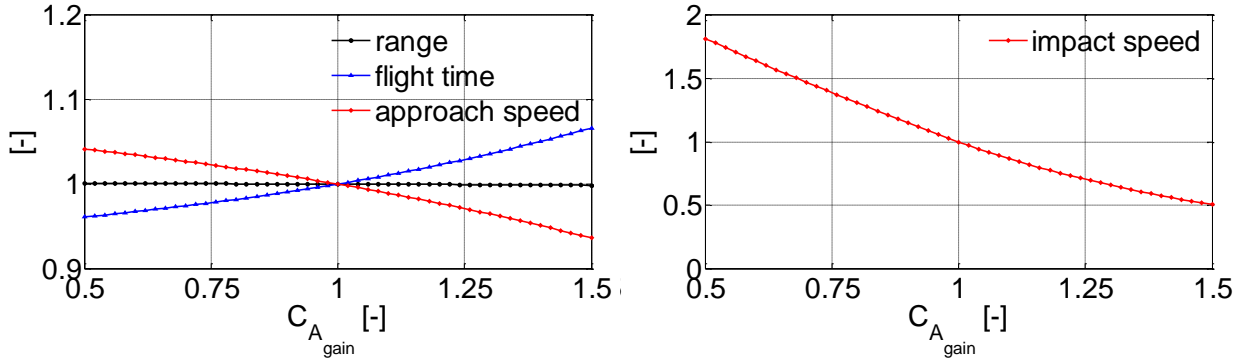


Figure 10: C_A Variation

A variation of C_A has a very small effect on the range. The range decreases with an increasing C_A by less than 0.5%. This phenomenon may be explained by small residence time of the vehicle within the atmosphere and the chosen trajectory inclination, making the horizontal flight range during reentry minimal. In contrast, the flight time increases almost linearly with increasing C_A to a maximum of 107%. Due to the increasing drag by raising C_A the reentry is decelerated. This is confirmed by the course of the impact speed, which decreases from 180% to 50% compared to the reference run over the examined period. The maximum lateral load factor is unaffected by C_A and is determined by the acceleration due to gravity.

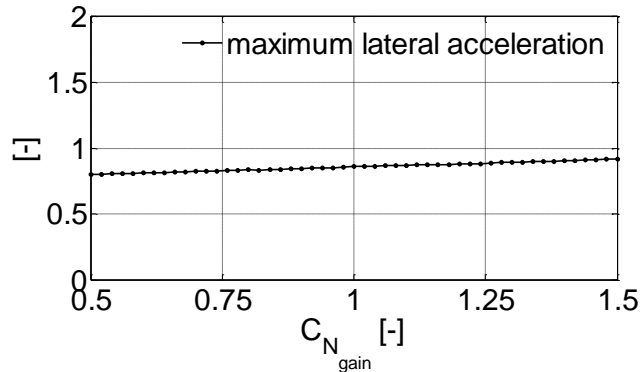


Figure 11: C_N Variation

A variation of the C_N and the three derivatives C_{lp} , C_{mq} , C_{nr} has no influence to range, flight time or approach speed. The maximum load factor in the reentry in the investigated interval results from the gravitational acceleration. An increase of C_N has direct impact on the oscillation of the inclination and leads to their gain, which results in an increasing lateral acceleration. Still maximal deviations from the impact point of the reference simulation yield ca. 9 m.

III.II Variation of mass properties

The variations of the mass are significant for the estimation of expected MRBM range at specified propulsion parameters and reentry deceleration of the vehicle. The mass of the reentry body was varied in the range of $\pm 10\%$ with an increment of 0.5%.

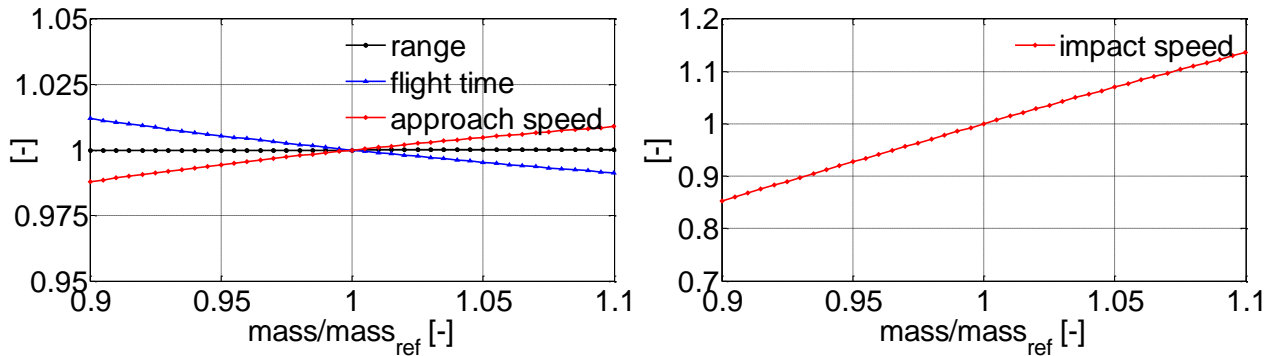


Figure 12: Mass Variation

Higher mass leads to a linear increase of the approaching speed. The range is unaffected by the mass variation. As a result the speed of approach rises due to falling flight time. The increasing mass in combination with a constant initial speed leads to a greater kinetic energy which is impressed on the re-entry at startup. With increasing mass the ballistic coefficient rises, which in particular affects the impact speed.

The maximum lateral load factor is virtually unaffected by the mass variation. Due to the aerodynamically undisturbed reentry the oscillation of the angle of attack has low magnitude, so that the measured values correspond to the percentage of acceleration due to gravity.

III.III Variation of AoA at the reentry

To investigate the effect of the angle of attack on reentry behavior, the initial incidence was varied from the reference track from 0° angle up to 180° with an increment of 2° . To enable a comparison of the flight paths, the elevation angle was changed in the same direction in order to achieve the same flight path angle for the trajectories.

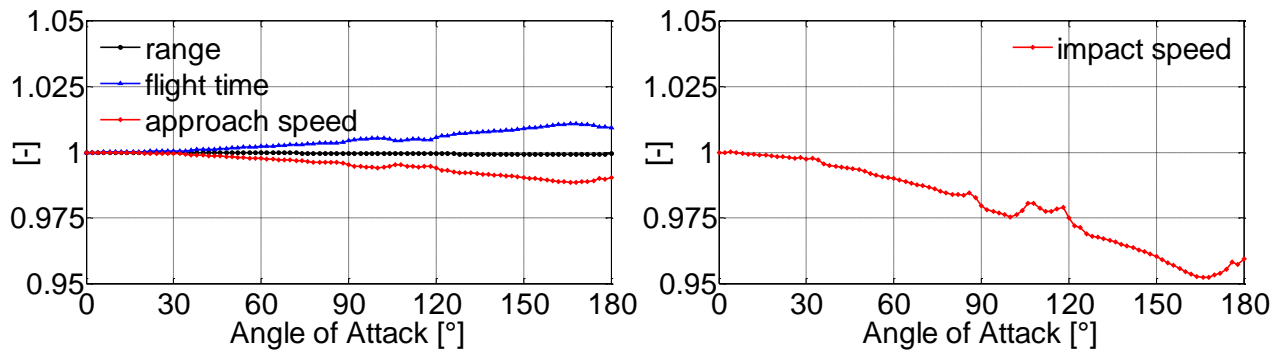


Figure 13: Angle of Attack Variation

With increasing angle of attack the flight time increases approximately linearly by about 1%, while the approaching speed decreases to the same extent. A greater influence has to be noted to the impact speed. This is due to the increasing angle of attack which comes along with increasing aerodynamic drag. This leads to a strong deceleration in deeper atmosphere layers.

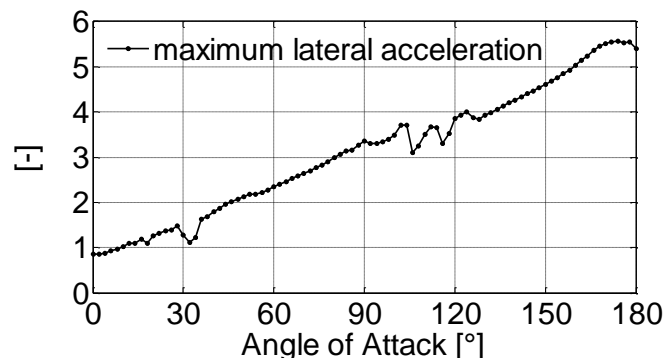


Figure 14: Angle of Attack Variation

With increasing angle of attack the maximum lateral load factor rises linearly and reaches a maximum factor of 5.5, compared to the reference case.

Stabilization effects dominate the RV movement for initial inclination angle of 20° and default conditions starts at altitudes below 100 km - Figure 15. The frequencies of the incidence oscillations increase continuously with altitude diminution yielding ca. 2.5 Hz between 40 and 30 km height.

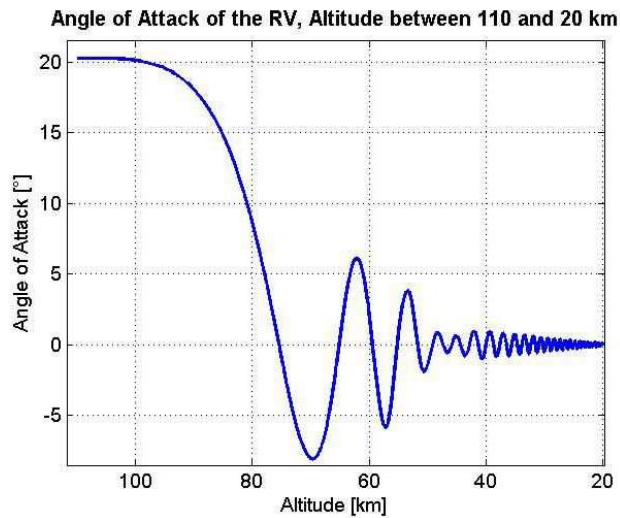


Figure 15: Angle of attack stabilization

Due to small asymmetry in the aerodynamic coefficients, first coupling effects in pitch and yaw axis occur at altitudes below ca. 60 km. In the reference sector of 40-30 km, lateral accelerations yield amplitudes of 5 m/s^2 and reach maximal values of $\pm 7 \text{ m/s}^2$ on altitudes between 30 and 20 km.

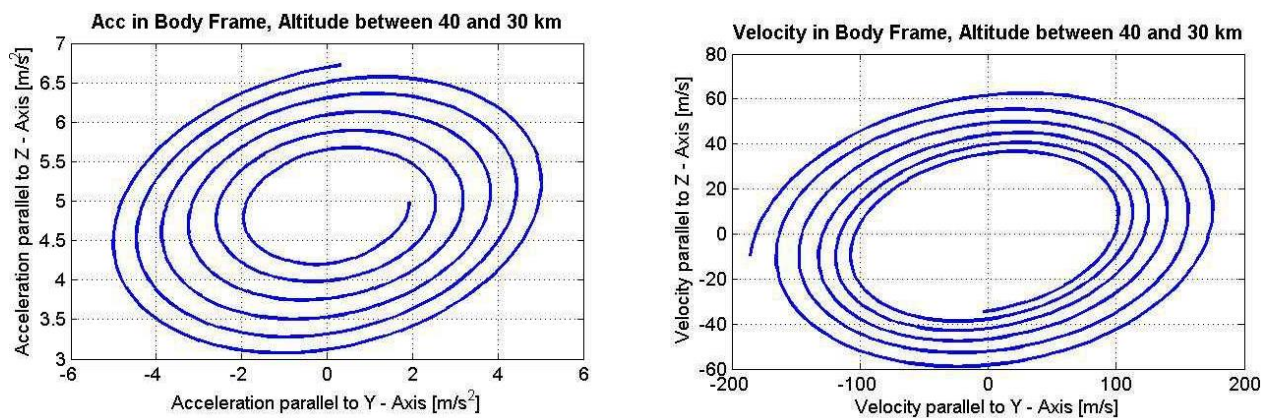


Figure 16: Acceleration and velocity in reference case, plane normal to undisturbed trajectory

The observation of lateral accelerations and velocities in the body frame gets imprecise with higher angles of attack concerning true flight path deviations within kinematic - or NED - frame. Still at small incidence angles total lateral accelerations may be picked as reference criterion for interceptor missile design. Maximal impact point deviations are also very small, reaching 65 m comparing to reference case.

III.IV Variation of Roll Rate

The roll rate was varied in the interval of 0 rad/s to 25 rad/s, respectively 8 Hz with an increment of 0.5 rad/s. With the examined boundary conditions there is no effect on the flight performance. Figure 17 shows angle of attack oscillation during reentry with roll rate of 1 Hz. Here, small coupling effects between the roll frequency and angle of attack oscillations occur, resulting in slightly higher amplitudes, following by larger lateral accelerations - Figure 18, compared to the reference case.

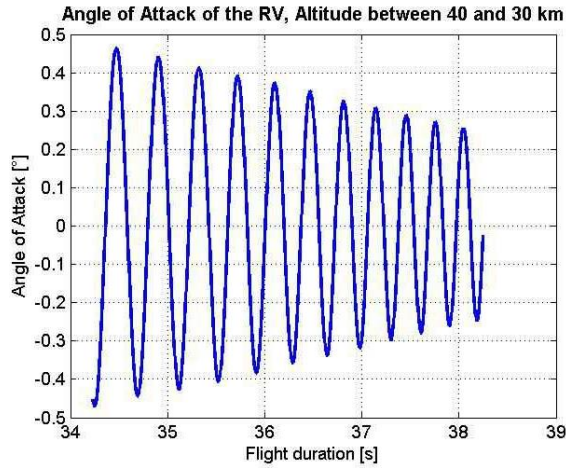


Figure 17: Angle of attack within considered altitude

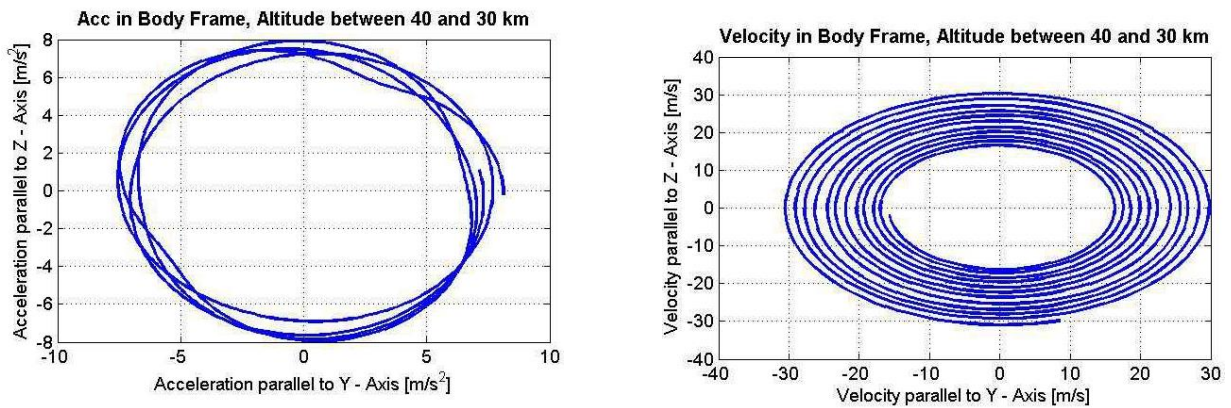


Figure 18: Acceleration and velocity in reference case, plane normal to undisturbed trajectory

III.V Variation of COG offset

Due to typically unknown detailed composition of RV, assumptions have to be made. Despite desirable geometrical symmetry, deviations in COG position may be intended to induce pitch and yaw oscillations during reentry. Thus offsets in x and y – directions from the reference case were simulated. Due to Steiner’s theorem, COG offset results in simultaneously adaption of mass moments of inertia.

The center of gravity of the reentry body in x-direction was varied in the range of $\pm 10\%$ with an increment of 0.5%. Under the examined boundary conditions, only small effects on flight performance, especially flight time, range and approaching velocity were observed.

Here, an initial displacement of the COG forward to the cone resulted in higher flight stability and lower energetic losses resulting from smaller angle of attack oscillations.

The COG displacement backwards to the body end reduces aerodynamic stability and thus raises tendency for angle of attack oscillations. Without coupling of initial parameters like roll rate, angle of attack incidence no significant lateral accelerations can be observed.

The center of gravity in y-direction was varied in a range of $\pm 10\%$, based on the caliber, with an increment of 0.5%.

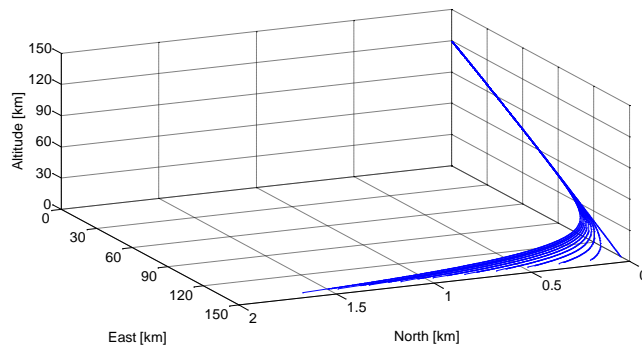


Figure 19: Trajectories y-COG offset

The impact on the range, flight time and approach speed is less than 1%. The lever between the aerodynamic center and center of gravity leads to a yaw movement, whereby a sideslip angle is established. The increased

aerodynamic drag results in a reduced impact velocity by up to 5%. Additionally the increased aerodynamic drag leads to an increasing flying time.

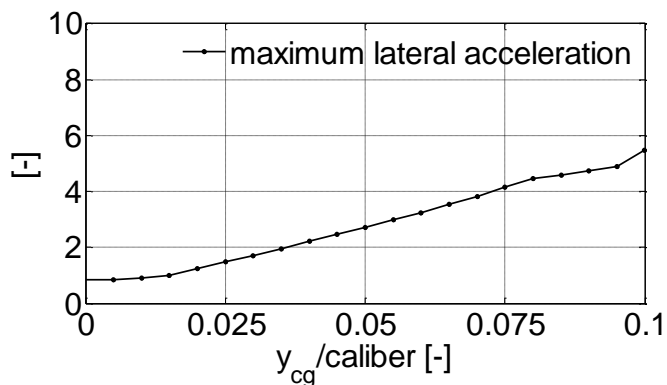


Figure 20: y-COG Variation

Due to the increasing sideslip angle with higher center of gravity offset, the maximum lateral acceleration in the reentry increases linearly and rises to a factor of 6.5 compared to reference case. The oscillation induction starts below 70 km height and the major effect will be reached at low altitudes, where the air density reaches its maximum, example Figure 21 and Figure 22.

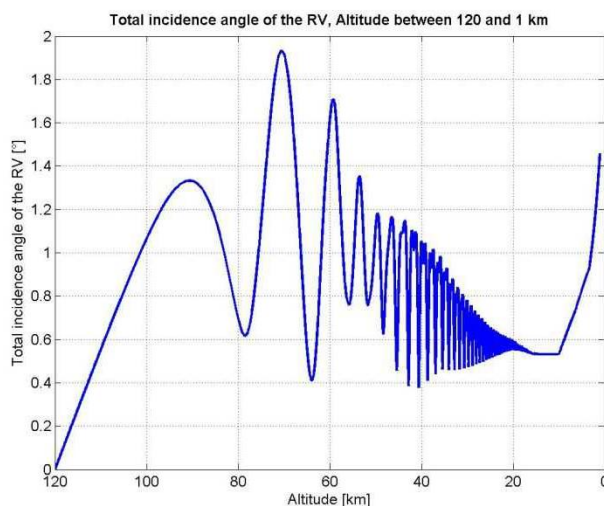


Figure 21: Total incidence angle at initial y-COG offset of 0.06 m (10% of the caliber)

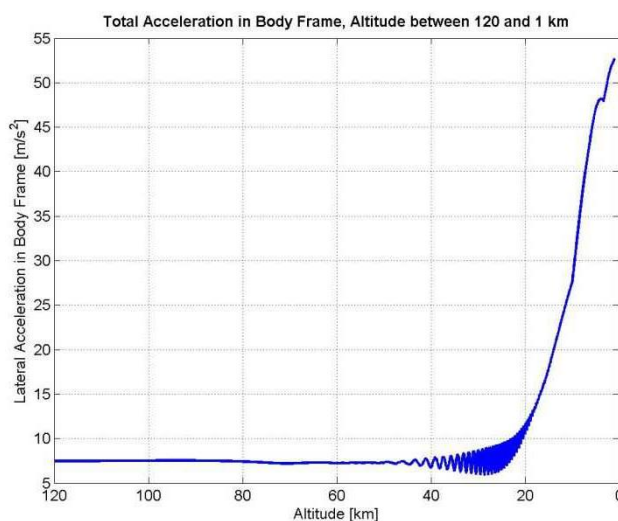


Figure 22: Total lateral acceleration in body frame at initial y-COG offset of 0.06 m (10% of the caliber)

The center of gravity position in z-direction was also varied in a range of $\pm 10\%$, based on the caliber, with an increment of 0.5%. Here, similar effects as with a y-COG position variation were observed.

The shift in the z-direction leads to a pitching moment due to the lever between center of gravity and aerodynamic center. A shift in positive z-direction creates a pitching up moment, which leads to an increase of range and flight time of approximately 2% and reduces the impact speed by 14% in comparison to the reference case. According to that a shift of the center of gravity in negative z- direction reverses the sign of the resulting moment. This

results in a pitching down moment, which decreases range and flight time. The impact speed increases by 8 % due to the shorter flight phase.

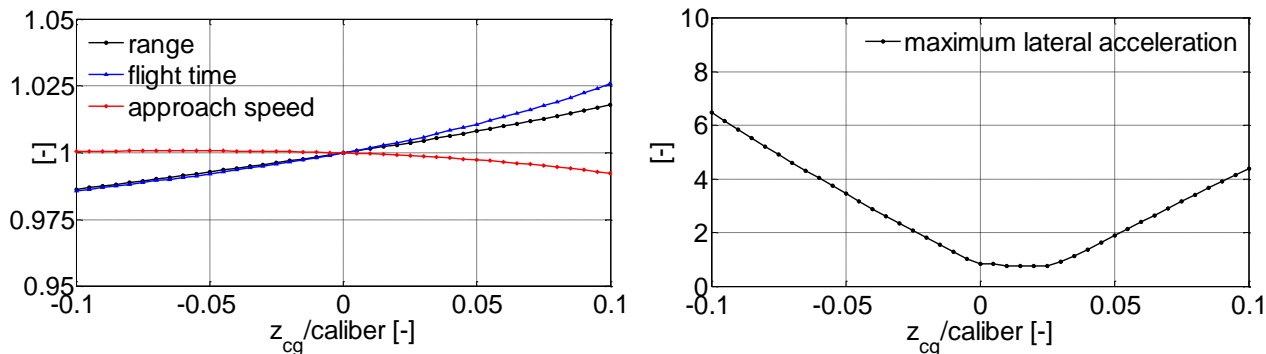


Figure 23: z-COG Variation

Well known deviation moments and forces on the reentry vehicle resulting from y- or z – COG displacement, may be used for the deception of missile defense systems, presuming precise attitude setting of the RV by post boost system and absence of roll-induced moments during reentry. In case of active COG position control systems combined with inertial navigation and guidance unit, both CEP values may be minimized and evasion maneuvers performed. At COG offsets of 0.06 m, range deviations of approximately 2.5 km in specific case may be achieved, without use of additional aerodynamic surfaces.

III.VI Coupling between Roll Rate and AoA

One of the simplest ways to induce lateral acceleration oscillations and hinder interceptor systems during the reentry is to give the RV an initial spin and incidence angle using the post boost system. Simulations with initial incidence angles of up to 40° and roll rates of 25 rad/s respectively 4 Hz were made. A clear tendency of increasing lateral accelerations with higher initial parameter values can be observed – example in Figure 24 at initial values for angle of attack of 10° and roll rate of 1 Hz with Figure 25 for initial AoA of 40° and roll rate of 4 Hz.

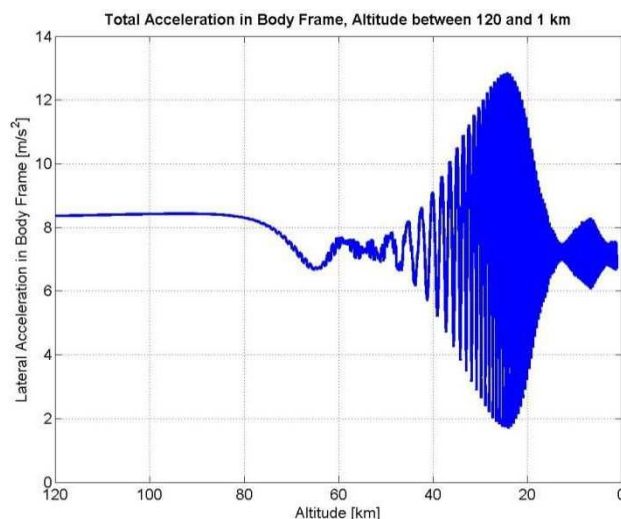


Figure 24: Total acceleration at initial angle of attack of 10° and roll rate of 1 Hz

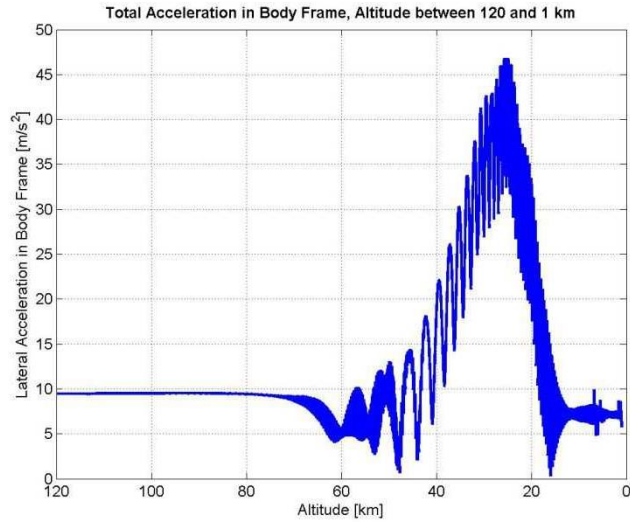


Figure 25: Total acceleration at initial angle of attack of 40° and roll rate of 4 Hz

During high frequency and incidence angles conditions, typical oscillation frequencies in the lateral acceleration can be observed. At altitudes between 40 and 30 km, these yield ca. 1.5 Hz and rise up to 6.5 Hz between 20 and 10 km.

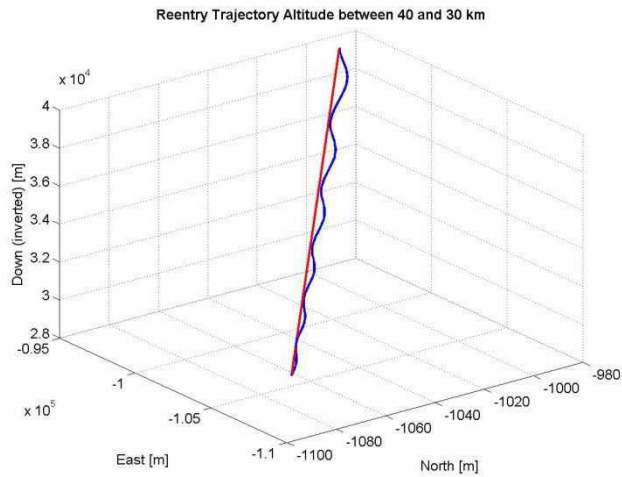


Figure 26: Reentry trajectory in NED frame

The blue curve in Figure 26 shows the reentry trajectory with a typical helix maneuver of the vehicle at altitudes between 40 and 30 km. The red curve represents ideal line between starting point at 40 km and ending point at 30 km height. The deviations from ideal line results from lateral accelerations during the stabilization phase of the vehicle. Calculating normal distances from the trajectory to ideal line yields values, given in Figure 27. While the major curvature with values of up to 15 m can be explained by gravitational and ballistic influence, small peaks result from lateral acceleration oscillations, yielding 2 - 4 meters with frequency of 1.5 Hz. Total displacements resulting from lateral accelerations in lower altitudes show values in ranges below 1 m, oscillating at higher frequencies.

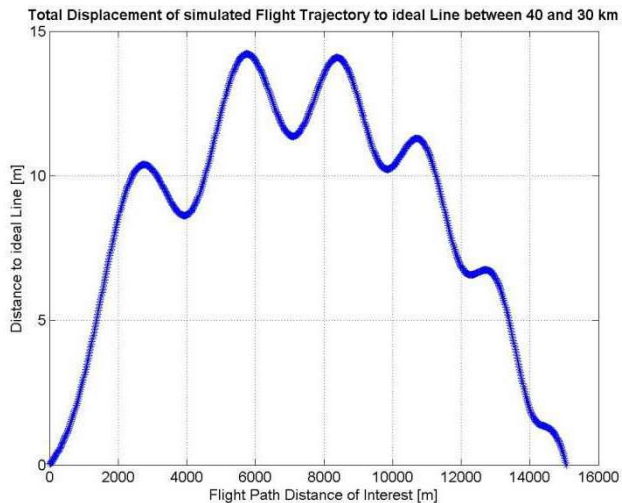


Figure 27: Total displacement of simulated trajectory to ideal line

By hindering the missile defense with setting of these initial values, a loss of CEP precision has to be taken into account. During simulations with initial incidence angle of 40° and roll rate of 4 Hz, deviations of up to 1 km on impact point were observed.

III.VII Coupling between y-COG, AoA and Roll Rate

The highest lateral accelerations could be achieved by setting the combinations of high initial y-COG offsets, moderate incidence angles, and small roll rates.

As described in previous chapter, y-COG offsets induce angle of attack oscillations at altitudes below ca. 80 km following by high lateral accelerations and stabilization effects below 20 km, where static incidence angles are achieved, Figure 21. In case of an initial angle of attack specification, oscillations occur with higher amplitudes, respective accelerations, example Figure 28 and Figure 29.

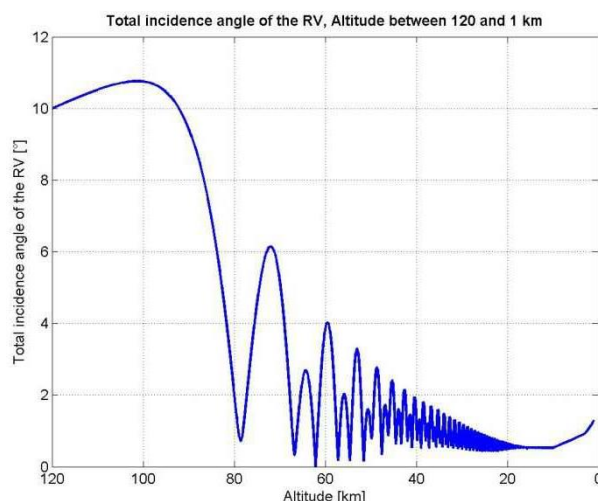


Figure 28: Total incidence angle at initial value of 10° and y-COG offset of 0.06 m

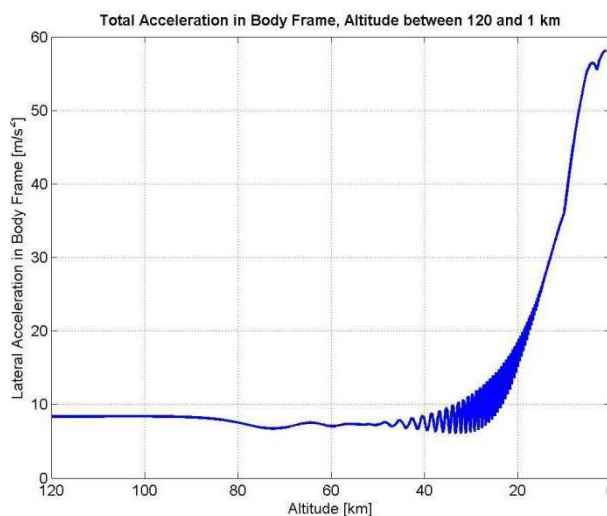


Figure 29: Total lateral acceleration in body frame at initial incidence angle of 10° and y-COG offset of 0.06 m

At initial y-COG offsets of 0.15 m, which correlates to 25% of the caliber, and incidence angles higher than ca. 16° , the reentry vehicle is unable to reach stable flight conditions and tumbles at altitudes between ca. 50 and 15 km. Here, the angle of attack reaches values over 90° , where longitudinal axis is positioned perpendicular to kinematic velocity. Total displacements between simulated trajectory and ideal line reach more than 50 m at altitudes between 40 and 30 km, leading high impact point deviations.

Initial roll rate settings stabilize the reentry maneuver and limit maximal lateral accelerations of the RV. Simulations with initial incidence angles of 10° , roll rate of 0.5 Hz and 0.15 m y-COG offset lead to complex lateral acceleration devolutions at high frequencies, Figure 30 and Figure 31. Fast Fourier transformation analyses on the presented acceleration course yield rapid frequency variation, without dominating values.

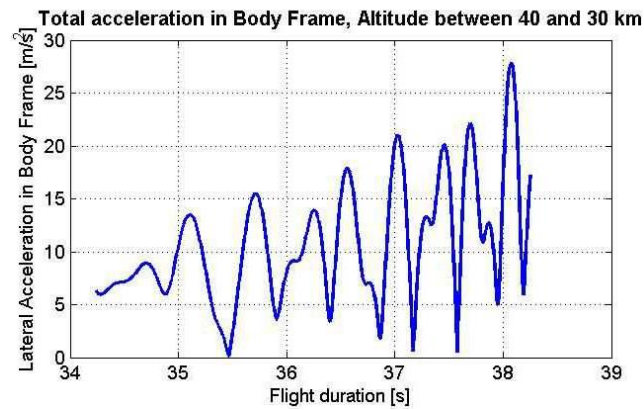


Figure 30: Total acceleration with initial incidence angle of 10° , roll rate of 0.5 Hz and y-COG offset of 0.15 m

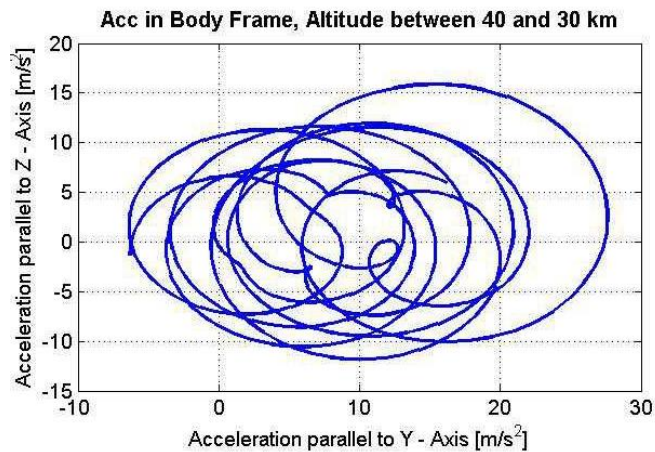


Figure 31: Acceleration in plane normal to undisturbed trajectory, with initial incidence angle of 10° , roll rate of 0.5 Hz and y-COG offset of 0.15 m

These simulation cases, leading the reentry vehicle to perform flight dynamic performance just within the stable regime where incidence angles stay below 90° , represent most dangerous circumstances. Even with small total distance deviations from the ideal trajectory in ranges below 0.5 m, yielding small CEP distances, high frequency oscillations may enhance seeker noise and thus disturb the interception maneuver.

IV Conclusions

The variation of flight parameters – roll rate and incidence angle resulting from release and inherent parameters of the reentry vehicle – COG position, mass moments of inertia can be analyzed considering two aspects. The first refers to the impact point of the reentry vehicle and second to the lateral flight dynamics, crucial for the development of countermeasure systems.

In comparison to the total flight range, trajectory deviation resulting from parameter variation may be neglected. Nevertheless, assuming the existence of internal steering devices, the manipulation of COG position may enhance the precision of intended impact point. Simulations on the RV geometry investigated here, showed lateral impact point shift of up to 2 km for COG displacement of 10%.

Considering lateral flight dynamics, acceleration over 50 m/s^2 was achieved in simulations, coupling inherent and initial flight parameters variation. Manipulations of initial roll rate in combination with incidence angle induce simple periodical acceleration oscillations, where typical frequencies can be observed and their motion evolution predicted by interceptor. Additional modification of inherent parameters yields a complex RV behavior without dominating frequencies, making the motion prediction and thus direct hit less feasible.

References

- [1] Weinand K., Dahlem K.-J., „Modellbildung und Simulation für den Fähigkeitserhalt und –aufwuchs der bodengebundenen Luftverteidigung“, SGW-Forum der DWT, Modellbildung und Simulation, Bonn, 2013

Corresponding translation:

„Modelling and simulation for capability preservation of surface based aerial defense“, SGW – Forum of DWT, Modelling and Simulation, Bonn, 2013

^[2] Ley W., Wittmann K., Hallmann W., „Handbuch der Raumfahrttechnik“, Carl Hanser Verlag München, 2011
ISBN: 978-3-446-4206-7

^[3] Hirschel E. H., „Basics of Aerothermodynamik“, Springer-Verlag Berlin Heidelberg, 2005
ISBN: 3-540-22132-8

^[4] Geulen G., „Freikonfigurierbare Parameteranalyse einer flugmechanischen Simulation“, Masterarbeit, MBDA GmbH, RWTH Aachen, 2015

Corresponding translation:

Geulen G., „Free Configurable Parameters Analysis of a Mechanical Flight Simulation“, Masterthesis, MBDA Deutschland GmbH, RWTH Aachen, 2015

^[5] Gallais P., „Atmospheric Re-Entry Vehicle Mechanics“, Springer-Verlag Berlin Heidelberg New York, 2007
ISBN: 978-3-540-73646-2